Exogenous origin of hydration on asteroid (16) Psyche: the role of hydrated asteroid families

C Avdellidou, M Delbo', A. Fienga

Monthly Notices
of the
ROYAL ASTRONOMICAL SOCIETY

MNRAS **475,** 3419–3428 (2018) doi:10.1093/mnras/sty017

Exogenous origin of hydration on asteroid (16) Psyche: the role of hydrated asteroid families

C. Avdellidou,[1]★ M. Delbo'[2]★ and A. Fienga[3]

[1] *Science Support Office, Directorate of Science, European Space Research and Technology Centre (ESA/ESTEC), NL-2201 AZ Noordwijk, the Netherlands*
[2] *Université Côte d'Azur, CNRS–Lagrange, Observatoire de la Côte d'Azur, CS 34229 – F-06304 NICE Cedex 4, France*
[3] *Université Côte d'Azur, CNRS–Geoazur, Observatoire de la Côte d'Azur, 250 Avenue de l' Observatoire – F-06250 Valbonne, France*

Accepted 2018 January 3. Received 2017 December 29; in original form 2017 August 23

ABSTRACT

Asteroid (16) Psyche, which for a long time was the largest M-type with no detection of hydration features in its spectrum, was recently discovered to have a weak 3-μm band and thus it was eventually added to the group of hydrated asteroids. Its relatively high density, in combination with the high radar albedo, led researchers to classify the asteroid as a metallic object. It is believed that it is possibly a core of a differentiated body, a remnant of 'hit-and-run' collisions. The detection of hydration is, in principle, inconsistent with a pure metallic origin for this body. Here, we consider the scenario in which the hydration on its surface is exogenous and was delivered by hydrated impactors. We show that impacting asteroids that belong to families whose members have the 3-μm band can deliver hydrated material to Psyche. We developed a collisional model with which we test all dark carbonaceous asteroid families, which contain hydrated members. We find that the major source of hydrated impactors is the family of Themis, with a total implanted mass on Psyche of the order of $\sim 10^{14}$ kg. However, the hydrated fraction could be only a few per cent of the implanted mass, as the water content in carbonaceous chondrite meteorites, the best analogue for the Themis asteroid family, is typically a few per cent of their mass.

Key words: minor planets, asteroids: individual: (16) Psyche.

1 INTRODUCTION

Throughout the last decades, study of the physical properties of the asteroid (16) Psyche has led to the demonstration that it is a peculiar body in our Solar system. It was spectroscopically classified as an M-type (Tholen 1989), a taxonomic class containing asteroids with geometric visible albedos between ∼0.1 and 0.2 and a generally featureless and slightly red reflectance spectrum, properties similar to those of the Fe/Ni metal (Gaffey et al. 2002). Therefore Psyche, the largest M-type asteroid and target of the National Aeronautics and Space Administration (NASA) space mission *Psyche* (Elkins-Tanton et al. 2017), is considered to be the Fe/Ni core of a differentiated body (or planetesimal) that was exposed by 'hit-and-run' collisions, capable of removing an asteroid's crust and mantle (Asphaug & Reufer 2014). The metallic nature of the asteroid is strongly supported by the value of its high radar albedo, 0.42 ± 0.1 (Shepard et al. 2010), which, along with the surface density, estimated at 3750 kg m^{-3}, suggests a 50 per cent macroporosity of the upper 1 m of subsoil (Ostro, Campbell & Shapiro 1985; Magri et al. 1999).

According to the Bus–DeMeo taxonomy (DeMeo et al. 2009), M-types are divided into the X_c, X_k and X_e classes of the X complex and thus Psyche is classified as an X_k asteroid in this modern taxonomy. Observations in the near-IR have shown features (1–3 per cent depth) in the pyroxene 0.9- μm region, with variation of the band centre and depth at different rotation phases (Hardersen, Gaffey & Abell 2005; Sanchez et al. 2017). Moreover, the pyroxene absorption band is persistent with rotation, although the signal is weak, meaning that silicates dominated by orthopyroxene are mixed with the metallic component of Psyche's surface (Sanchez et al. 2017). This observation could indicate an endogenous origin of the silicates, but an exogenous origin of these silicates cannot be ruled out, as we see in the case of Ceres and the presence of enstatite material (Vernazza et al. 2017).

A striking interesting result is the detection of the 3-μm absorption feature (Takir et al. 2017) in spectra of the asteroid. This was detected in four different rotation phases, consistent with the presence of OH- and/or H_2O-bearing phases. The shape of the 3-μm feature is similar to that of other outer Main Belt asteroids and corresponds to the so-called 'sharp group' connected to CM-like phyllosilicates (Takir & Emery 2012; Rivkin et al. 2015). Moreover, in one data set the feature is similar to that observed on the asteroid Ceres (Ceres-like group: Takir & Emery 2012). This new

★ E-mail: chavdell@gmail.com (CA); marcodelbo@gmail.com (MD)

discovery eventually added Psyche to the list of M-types with 3-μm features (Merényi et al. 1997; Rivkin et al. 2000).

The presence of hydration sets new constraints on the study of asteroids. If Psyche has an iron core, then any hydration cannot be endogenous but must have been deposited on the surface by another process. Recently, it has been demonstrated (McCord et al. 2012; Turrini et al. 2014, 2016) that the dark regions on asteroid (4) Vesta are the result of deposition of exogenous material via impacts. This cannot be explained as exposition of mantle material after impacts, since these events cannot be energetic enough to excavate to such depths. In addition, the previous model can also verify that the presence of submicroscopic siderophile elements, such as exogenous inclusions, originated from hypervelocity impacts on Vesta (see Turrini et al. 2014 and references therein).

The deposit of exogenous materials on the surface of Ceres can also explain recent observations of this dwarf planet, which were carried out from the Sofia airborne observatory (Vernazza et al. 2017). Contamination of asteroid surfaces from the impact of materials originating from other asteroids is also consistent with recent laboratory findings, where it has been shown that a significant amount of the impactor material can be preserved on the target (Daly & Schultz 2015, 2016; Avdellidou et al. 2016, 2017). More specifically, it has been shown that the impactor is not pulverized and can be implanted into and around the impact crater at impact velocities $\lesssim 2\,\mathrm{km\,s^{-1}}$ (Avdellidou et al. 2016, 2017).

Here, we study the potential sources of impacts that can deliver OH- and or H_2O-bearing minerals on Psyche. The intrinsic impact probability with all possible impact velocities between all possible pairs of asteroids in the Main Belt is 2.86×10^{-18} impact $\mathrm{km^{-2}\,yr^{-1}}$ (Bottke et al. 2005), resulting in an average impact probability of about 3.6×10^{-8} impact $\mathrm{Myr^{-1}}$ using the most recent estimation for Psyche's size (diameter $D = 225.5$ km; see Section 2) and sizes of impactors of about 1 km in diameter. As the total impact probability is proportional to the time and the number of available projectiles, this requires a large number of impactors ($\sim 6 \times 10^3$ or more) carrying hydrated minerals and/or water in order to have some deposits on this asteroid over the 4.6-Gyr long age of the Solar system (which is also likely the age of Psyche). While the number of asteroids with spectroscopically measured hydration is growing, their number is very limited: there are 48 known asteroids that display the 3-μm absorption feature (Rivkin 1997; Rivkin et al. 2000, 2015; Rivkin & Emery 2010; Takir & Emery 2012) and 28 asteroids are Ch and Cgh types (see the data base of Delbo' et al. 2017, at mp3c.oca.eu), indicative of the presence of the 0.7-μm absorption band. The 0.7-μm feature indicates the presence of phyllosilicates, likely due to aqueous alteration (Vilas & Gaffey 1989).

In order to have a large number of projectiles, our working hypothesis is that these materials were deposited on the surface of Psyche by impacts of asteroids that were members of collisional families, whose asteroids have a signature of hydrated minerals and/or water ice. After the break-up of an asteroid parent body, a large number of small fragments – the family asteroid members – are produced, thus creating an impactor population large enough to overcome the aforementioned low impact probabilities. In addition, it is known that members of asteroid families are broadly compositionally homogeneous, implying that if hydration is observed for one member – typically the family parent body – then it is reasonable to assume that all members of the family are hydrated.

As we shall demonstrate, asteroids belonging to the so-called background, namely those that are currently not linked to any known family, also impacted Psyche. There is growing evidence that the background is composed mostly by members of families that are yet to be identified (Delbo' et al. 2017; Tsirvoulis et al. 2017; this has also been predicted by Zappala & Cellino 1996). However, at the moment we do not know these 'missing families'. Therefore asteroids of the background, in contrast to members of families, do not have a composition link between them or with common parent bodies. This makes it difficult to estimate the amount of hydrated material, if any, that impactors from the background population have delivered to Psyche.

Our work is structured as follows. In Section 2 we discuss some relevant physical characteristics of Psyche, such as its mass and size; in Section 3 we present the potential asteroid family sources of the impactors; in Sections 4 and 5 we show the method followed and calculate the amount of implanted mass, while Sections 6 and 7 give a discussion and the main conclusion of the results. There, we also show that the so-called asteroid background with low albedo contributes to implanting mass on Psyche. However, this background, which consists of asteroids currently not associated with any family, cannot be proven to be hydrated, as a genetic relation to the few hydrated bodies in the Main Belt is not yet established.

2 PSYCHE BACKGROUND

The estimation of the bulk density of Psyche obviously depends on the measurement of the object's dimensions. Several works have focused on measurement of the size of Psyche using *IRAS* observations (Tedesco et al. 2002), *WISE* data (Masiero et al. 2012), *Akari* thermal infrared data (Usui et al. 2011), speckle interferometry (Cellino et al. 2003), adaptive-optics imaging (Drummond & Christou 2008), radar imaging (Shepard et al. 2008) and the combination of the available shape model (Kaasalainen, Torppa & Piironen 2002) with occultations (Ďurech et al. 2011) and thermophysical models applied to long-baseline, ground-based interferometric observations obtained from the European Southern Observatory (ESO) Very Large Telescope Interferometer (VLTI: Matter et al. 2013). However, all the above measurements lead to densities spanning a wide range of values from $1800 \pm 600\,\mathrm{kg\,m^{-3}}$ (Viateau 2000) to $6580 \pm 580\,\mathrm{kg\,m^{-3}}$ (Kuzmanoski & Kovačević 2002), implying different composition models, and thus are not conclusive. A recent work based on radar-delay-Doppler, adaptive optics and stellar occultations found the diameter $D_{\mathrm{eff}} = 226 \pm 23$ km, with exact dimensions $279 \times 232 \times 189\,\mathrm{km^3} \pm 10$ per cent (Shepard et al. 2017), which is in almost perfect agreement with a simultaneous work that constrained Psyche's effective diameter to be $D_{\mathrm{eff}} = 225 \pm 4$ km, also using adaptive optics and occultations (Hanuš et al. 2017). Combining this D_{eff} with the most recent mass estimations (Carry 2012; Fienga et al. 2014), the bulk density is calculated to be between 3500 and $4500\,\mathrm{kg\,m^{-3}}$ (Hanuš et al. 2017; Shepard et al. 2017). All data combinations of these physical properties, obtained from the latest observations, are given in Table 1.

2.1 High- and low-density scenarios

If we consider for the bulk density the value $4500\ \mathrm{kg\ m^{-3}}$, which is one of the highest measured in the asteroid population out of those asteroids with good quality of data (see Carry 2012), it will strengthen the hypothesis that Psyche could be an exposed metal core of a differentiated asteroid (Elkins-Tanton et al. 2017). According to the models of asteroid differentiation, the process that led to the formation of Psyche happened very early. Considering Psyche's current diameter, $D_{\mathrm{eff}} = 226$ km (Shepard et al. 2017), the Psyche parent body (PPB) was supposed to be ∼500 km in diameter

Table 1. Estimated masses and diameters for Psyche, along with their derived bulk densities. For each value, the corresponding reference is given.

Case	Mass $\pm 1\sigma$ (10^{19} kg)	Diameter $\pm 1\sigma$ (km)	Bulk density $\pm 1\sigma$ (kg m^{-3})
1.	2.72 ± 0.75 (Carry 2012)	226 ± 23 (Shepard et al. 2017)	4530 ± 1280 Shepard et al. (2017)
2.	2.22 ± 0.36 (Fienga et al. 2014)	225 ± 4 (Hanuš et al. 2017)	3700 ± 630 (Hanuš et al. 2017)
3.	2.54 ± 0.26 (Viswanathan et al. 2017)	225.5 ± 4*	4200 ± 490**
4.	2.21 ± 0.21	225.5 ± 4*	3500 ± 400**

*This value is calculated in this work as an average of Cases 1 and 2.
**Recent calculations, presented in this work.

and have suffered severe 'hit-and-run' impact events capable of removing all crust and mantle, exposing the core (Elkins-Tanton et al. 2016). In addition, Psyche should have ∼40 per cent macroporosity, if we assume that it is made of blocks of iron/nickel with a density around 7500 kg m^{-3}. In that case, the core itself was possibly destroyed and re-accumulated, implying a severe collisional history. When an asteroid is disrupted catastrophically, with a remaining mass ≤50 per cent of the initial one, after a collision with another body, an asteroid family is formed. If the collision happened in the Main Belt, a family of asteroid fragments should be in the region of Psyche; however, no family related to Psyche has been found yet (Davis, Farinella & Marzari 1999). One possibility to solve this issue is that the potential Psyche asteroid family was created at an early time, e.g. within the first 500 Myr of Solar system history (Davis et al. 1999). This would allow the family fragments to be ground down by collisional evolution and be unobservable today. The same models show that, even in this case, today there should be several surviving fragments having diameters around 20 km and above the detection limit. There is a lack of primordial asteroid families in the Main Belt (Brož et al. 2013; Spoto, Milani & Knežević 2015), very likely due to the classical methods that are used to identify them. The hierarchical clustering method (HCM) is not sensitive enough to find old and dispersed families, as it searches for asteroids forming compact groups in orbital element space (semi-major axis, eccentricity and inclination). A new approach has been proposed and implemented with success (Walsh et al. 2013; Delbo' et al. 2017), as it is able to distinguish very old families, having eccentricities and inclinations dispersed in space. Therefore the possibility of the absence of a Psyche family could be due to searching biases. However, this may be an unlikely hypothesis, because A-type asteroids that could represent mantle material (almost pure olivine) from differentiated bodies do not exist extensively in the orbital space related to Psyche, but instead are distributed randomly in the Main Belt (Davis et al. 1999; DeMeo et al. 2015). In order to study this puzzling small body further, NASA is sending a new Discovery Mission to Psyche. The main goal is to get insight into whether it is a core of a parent body and understand the procedures of differentiation, making all the above questions more valid than ever. The alternative theory is that Psyche is a planetesimal that bears primitive unmelted material (Elkins-Tanton et al. 2016).

However, more recent estimations give lower values for the mass of Psyche. Specifically, here we present results for the density of Psyche using masses that were measured from gravitational perturbations by Mars (construction of the planetary ephemerides INPOP17a, see Viswanathan et al. 2017). The orbit of Mars is significantly perturbed by asteroids of the Main Belt and lately the masses of the most perturbing asteroids have been estimated using navigation data of Mars orbiters (Standish & Fienga 2002; Somenzi et al. 2010; Folkner et al. 2014). However, such mass determinations are sensitive to the weighting scheme used for the construction of each planetary ephemeride and, consequently, one should expect an uncertainty of at least 10 per cent in the mass of Psyche. From such observations, densities for this specific asteroid were found to be between 3500 and 4200 kg m^{-3}.

Using the most conservative scenario for the bulk density, 3500 kg m^{-3}, if Psyche is the remnant of an Fe/Ni core with a block density of 7500 kg m^{-3} then the body should still have almost 55 per cent macroporosity. From older statistics (Carry 2012), it was shown that asteroids with mass of about 10^{20} kg are solid bodies with almost no macroporocity. This implies that Psyche, with $M \sim 2 \times 10^{19}$ kg, could be at the borderline of this estimation and both scenarios, i.e. solid or porous body, could be marginally valid. One of the key parameters through which to start studying the iron core mystery is to consider the presence of OH/H_2O on its surface. If we assume the iron core scenario, then any water should be exogenous and implanted by a number of impacts.

In this work we are going to consider Case 3 from Table 1. $D_{\rm eff}$ is selected as the average of the most recent observational works (Shepard et al. 2017; Hanuš et al. 2017), while the mass is one of the latest estimations (Viswanathan et al. 2017) derived from close encounters with Mars, giving a bulk density of 4200 kg m^{-3} and escape velocity $v_{\rm esc} = 0.179$ km s^{-1}.

3 EXOGENOUS REPOSITORIES

Following our hypothesis that the exogenous water and/or hydrated material on Psyche come from impactors that are members of asteroid families, we first investigate which of the known families contains members with water and/or hydrated minerals. To do so, we retrieve from the literature all asteroids with a 3-μm band of any type (sharp, round, Ceres and Europa type: e.g. Takir & Emery 2012; Rivkin et al. 2015, etc.). We then consider only those that are part of a family, using the family list and the asteroid membership of Nesvorny, Broz & Carruba (2015). These are the families of (2) Pallas, (10) Hygiea, (24) Themis, (31) Euphrosyne, (137) Meliboea, (153) Hilda and (363) Padua (see Table 2). In the following, for each of these families, we present relevant characteristics, identify and remove interlopers and study their size frequency distribution (SFD), which we also extrapolate to sizes smaller than the currently observable completeness size in the Main Belt. This is required because catalogued family classification is, in general, conservative, in order to avoid including background objects and to maintain good separation in orbital elements between different families (Milani et al. 2014).

3.1 Rejection of interlopers and size distributions of families

As a first step, we try to understand whether any of the hydrated family members is an interloper to its family. For this reason, we check whether the hydrated asteroids are within the Yarkovsky boundaries (Vokrouhlický et al. 2006) of their family. Family members

Table 2. Main belt asteroids with a detected 3-μm band that are also members of families. These families are thus potential sources of hydrated impactors on Psyche, according to our working hypothesis. Note that, since we find that (110) Lydia is an interloper inside the Padua family (see text), we reject this family as a source of hydrated impactors. The asteroids with a 3-μm band that are not members of families are not reported in this table.

Asteroid family	Hydrated members
Themis/Beagle	(24) Themis, (90) Antiope, (104) Klymene
Hygiea	(10) Hygiea, (52) Europa
Euphrosyne	(31) Euphrosyne
Hilda	(153) Hilda
Meliboea	(511) Davida
Pallas	(2) Pallas
Padua (rejected)	(110) Lydia

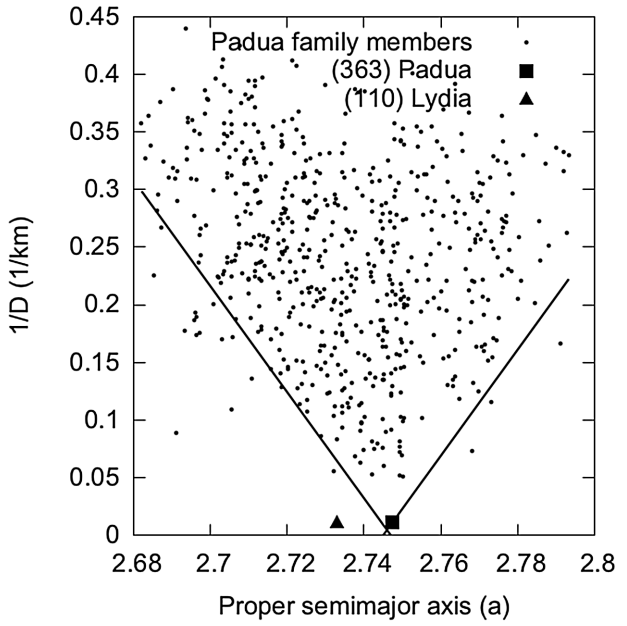

Figure 1. Asteroid (110) Lydia (triangle), which has a very similar diameter to (363) Padua, resides outside the V shape of the family. For this reason, along with the spectral and albedo differences, we do not consider it as a member of the Padua family.

form a V shape in a versus $1/D$ space, where a is the orbital semimajor axis and D is the asteroid diameter, due to the Yarkovsky non-gravitational forces. The use of this V shape in the a versus $1/D$ space to constrain the family members better has already been proposed and used as a method in several works (Walsh et al. 2013; Nesvorny et al. 2015; Bolin et al. 2017; Delbo' et al. 2017).

In the case of the Padua family, we can clearly identify the hydrated asteroid (110) Lydia as an interloper. In fact, as seen in Fig. 1, Lydia is far from the inward border of the V shape. The average albedo of the Padua family is $\langle p_V \rangle = 0.058$ and the standard deviation is 0.024. The albedo of (110) Lydia is 0.17 ± 0.02, which is more than 3σ away from the average albedo of the Padua family. On the other hand, the albedo of (363) Padua is 0.053, matching the average value perfectly. An additional reason that allows us to reject (110) Lydia from the family is that it has a different spectral classification: (363) Padua is a member of the C complex, while (110) Lydia is classified as an M type (or X_k type). Since no other Padua family member has a detected 3-μm band, we exclude this family as a potential source of hydrated impactors on the surface of Psyche.

Table 3. The slope α of each family is calculated by fitting a power law to the observed SFD up to the completeness limit (D_{17}), the actual value of which depends on the average albedo of the family members.

Asteroid family	$<p_V>$	N_{17}	α	D_{17}(km)
Themis	0.069	4535	−1.52	2.00
Hygiea	0.072	4837	−2.30	1.97
Euphrosyne	0.060	2035	−2.91	2.21
Hilda	0.051	409	−1.99	2.34
Meliboea	0.066	444	−1.56	2.06
Pallas	0.142	128	−1.32	1.40

The cumulative size frequency distributions (SFDs) are obtained using the same data base of asteroid physical properties of Delbo' et al. (2017). If the diameter is not reported in the literature, we calculate it from $D(\mathrm{km}) = (1329/\sqrt{\langle p_V \rangle}) \times 10^{-H/5}$ (see Harris 1998 and references therein) where $\langle p_V \rangle$ is the average albedo of the family members and H the absolute magnitude of each object.

The observed populations of the families, however, are not complete, due to observational biases, as smaller asteroids become more difficult to detect by telescopic surveys. The current limit of completeness of catalogued Main Belt asteroids is $H \sim 17$ (Jedicke et al. 2015; Denneau et al. 2015). Therefore we consider the SFDs of the families as complete for $H < 17$. This H limit corresponds to the diameter limit D_{17}, the value of which depends on the average albedo of the family (see Table 3). We assume that the cumulative number of asteroids down to any diameter $D < D_{17}$ is given by

$$N = N_{17} D^{a} D_{17}{}^{-a}, \quad (1)$$

where D_{17} is the diameter at $H = 17$ and N_{17} the total number of bodies with $H < 17$. The slope α is obtained by fitting a power law of $N(D) = kD^{\alpha}$ (which is a straight line in a $\log N$ versus $\log D$ space) to the known population for $H < 17$ and is negative as $\mathrm{d}N/\mathrm{d}D$ increases for decreasing D.

3.2 Themis and Hygiea families

The Themis and Hygiea asteroid families are considered as the major contributors to impactors on Psyche, because they have the most numerous family members and the 3-μm band is detected not only for the parent body but for several objects per family.

Themis is a family of the outer Main Belt, ranging from 3.02–3.24 au in proper semimajor axis (a_p), between 0.0116 and 0.0404 in proper sin inclination ($\sin(i_p)$) and between 0.1115 and 0.1862 in proper eccentricity (e_p). It was formed 2.5 ± 1.0 Gyr ago (Brož et al. 2013); however, a recent estimate gives the age limits for Themis to be between 2.4 and 3.8 Gyr (Spoto et al. 2015). The majority of Themis family members belong to the C complex (Florczak et al. 1999; de León et al. 2012; Fornasier et al. 2016). This family is located in an area where hydration (Florczak et al. 1999; Takir & Emery 2012) and water ice have been found. The observation of the 3-μm band on (24) Themis, the family parent body, could be explained by 4 per cent of water ice on the surface (Rivkin & Emery 2010) that is additionally distributed over a wide range of latitudes (Campins et al. 2010), making it the first C-type asteroid to have a water-ice layer with organic compounds on its surface. The presence of water ice in the Themis family is consistent with the discovery of so-called Main Belt Comets (MBCs: Haghighipour 2009; Hsieh et al. 2012; Hsieh 2014) within this family. The most probable explanation for the activity of MBCs is that the

latter is driven by sublimation of water ice and other volatiles. Apart from the MBCs, other asteroid members of the family were found to have both the 'round' 3-μm water-ice band, e.g. (90) Antiope (Hargrove et al. 2015), and 'sharp' absorption, e.g. (104) Klymene (Takir & Emery 2012), showing the presence of OH in the mineral lattice (Jones 1988). Additional evidence that these objects could have high water content comes from the densities of three Themis members, (24) Themis, (90) Antiope and (379) Huenna, that have very low density values, around 1280–1800 kg m^3 (Descamps et al. 2007; Carry 2012). Geophysical evolution models for (24) Themis (Castillo-Rogez & Schmidt 2010) have suggested that the parent body had accreted from ice mixed with carbonaceous material and before the time of the break-up – forming the Themis family – it differentiated, implying that more asteroid members of the family should contain water ice. Recent compositional characterization of Themis family members confirms the above scenario. Assuming a parent body of 400 km in diameter, its accretion should have happened about 4 Myr after Calcium-aluminium-rich inclusions and aqueous alteration happened in the core and not in the outer shell. Thus a number of Themis members should consist of ice and anhydrous silicates, while others should consist of hydrated minerals (Marsset et al. 2016). This scenario is consistent with a previous study that showed that two-thirds of C-complex asteroids of the outer Main Belt should have undergone aqueous alteration (Jones et al. 1990). The mean geometric visible albedo of the family is $\langle p_V \rangle = 0.069$, with a root-mean-square (rms) of 0.02. According to the family classification of Nesvorny et al. (2015), it has a total of 4633 members.

The family of Hygiea is younger than that of Themis and was formed after a cratering collisional event 2.0 ± 1 Gya (Brož et al. 2013; the family age of ∼1.3 ± 0.3 Gyr from Spoto et al. 2015 agrees with the Brož et al. 2013 estimates). This family is also located in the outer Main Belt ($3.029 < a_p < 3.242$ au), where the inclinations of its members ($0.0691 < \sin(i_p) < 0.1167$) are larger than those of Themis family members, but the eccentricities of the two families ($0.0941 < e_p < 0.1722$) almost overlap. For (10) Hygiea itself and (52) Europa, the absorption band has been detected. However, according to the current classification (Takir & Emery 2012), (10) Hygiea has a band typical of the Ceres group, while (52) Europa has a different band, constituting the 'Europa group'. The mean geometric visible albedo $\langle p_V \rangle$ of the family is 0.07 with an rms of 0.03 and it has a total of 4852 members (Nesvorny et al. 2015).

4 COLLISIONAL AND CONTAMINATION MODEL

Having identified the asteroid families that are potential sources of impactors with a 3-μm band, in this section we describe the method to calculate the amount of implanted material on asteroid Psyche from each of these sources. We broadly follow the technique developed to explain the dark deposits on the surface of asteroid (4) Vesta (Turrini et al. 2014), which includes a collisional and contamination model.

The number of impact events on Psyche for a specific diameter bin of width dD of the impactor population can be calculated as (O'Brien & Sykes 2011)

$$\mathrm{d}N_\mathrm{I} = P_\mathrm{P} A \frac{\mathrm{d}N}{\mathrm{d}D} T \, \mathrm{d}D, \quad (2)$$

where P_P is the intrinsic impact probability (per year and per km^2) on Psyche, A the cross-section of the target and of an impactor of size D, dN/dD the differential size distribution of the impactor population and T the time interval. The cross-section A is calculated as

$$A = (R_\mathrm{P} + 0.5D)^2 \sim R_\mathrm{P}^2, \quad (3)$$

where D is the diameter of an impactor and $R_\mathrm{P} = 112.5$ km is the current estimation for the radius of Psyche (Table 1).

The intrinsic impact probability of each source of impactors on Psyche, P_P, depends on the orbits of the target and of the impactors. We calculate P_P using the algorithm of Wetherill (1967), which, given the semimajor axis, eccentricity and inclination of the orbits of two asteroids (a target and an impactor) and assuming that the mean anomaly, argument of perihelion and longitude of the ascending node have a uniform probability distribution over the interval 0–2π, computes which fraction of these angles corresponds to the two objects being closer to each other than 1 km. Next, the algorithm translates this fraction into an intrinsic collision probability per km^2 and per year (P_P) using the orbital periods of the two objects and assuming that they are not in resonance with each other. For each possible impact configuration (e.g. when the target and projectile are closer than 1 km), the algorithm also calculates the mutual (impact) velocity V. In a final step, the probabilities of all possible impact configurations are summed and the code determines an average impact velocity. We apply this algorithm to estimate the value of P_P and V between Psyche and each family member. For each family, we average the values of P_P and of V among its members (Table 4).

For T, we use the estimated ages of the families taken from the literature. In some cases the age is not well-determined, thus we perform an estimation of the number of impacts on Psyche and the amount of implanted material for each age case (see Table 5). In particular, we consider an upper and a lower limit for the ages of the Themis, Hygiea and Euphrosyne families. We follow a scenario in which a family contributes to the impactor flux on Psyche throughout the family lifetime T from equation (2), which is equal to the family age.

The implanted mass m is a fraction f of the impacting mass M on Psyche (Svetsov 2011). The value of f is given by

$$f = (0.14 + 0.003V) \ln v_\mathrm{esc} + 0.9V^{-0.24}, \quad (4)$$

where $v_\mathrm{esc} = 0.179$ km s^{-1} is the escape velocity from Psyche. For the value of the impact velocity V, we take the average impact velocity of each family obtained in the previous step, given in Table 4.

The number of impacts on the target is governed by Poisson statistics and is therefore affected by an uncertainty of the order of the square root of the number of calculated impacts. In order to take this into account, we calculate, for each asteroid family, the number of objects that are needed in order to give five or more impacts on Psyche during their lifetime. This translates to 99.9 per cent probability of having impact events and is calculated from the cumulative

Table 4. Average impact probabilities and collisional velocities of the source families on Psyche. The fraction of retained mass depends on the impact velocity V.

Asteroid family	$<P_\mathrm{P}> \pm \sigma$ (yr^{-1}km^{-2})	$<V> \pm \sigma$ (km s^{-1})	f
Themis	$7.9 \pm 1.0 \times 10^{-18}$	3.0 ± 0.1	0.41
Hygiea	$4.1 \pm 0.53 \times 10^{-18}$	3.1 ± 0.2	0.40
Euphrosyne	$2.19 \pm 0.53 \times 10^{-18}$	8.8 ± 0.3	0.22
Hilda	$5.8 \pm 5.8 \times 10^{-19}$	2.0 ± 2.0	0.49
Meliboea	$2.5 \pm 0.44 \times 10^{-18}$	5.6 ± 0.2	0.30
Pallas	$1.7 \pm 0.13 \times 10^{-18}$	10.7 ± 0.2	0.19

Table 5. Family ages from the literature (Age) and adopted (T) in our model to calculate the number of impact events on the asteroid Psyche. For Hygiea, Themis, and Euphrosyne, we run our model considering two possible T values for their age: high (H) and low (L). The implanted masses are calculated for the two parts of their SFDs (see the text for further details). The mass range from the families of Themis, Hygiea and Euphrosyne is calculated for a maximum (H) and minimum family age (L).

Asteroid family impactor source	Age	Reference	T	$D_{\rm lim}$	D^*	Implanted mass $D > D_{\rm lim}$	Implanted mass $D \leq D_{\rm lim}$
	(Gyr)		(Gyr)	(km)	(km)	$\times 10^{13}$ (kg)	$\times 10^{13}$ (kg)
Themis (H)	2.45–3.8 ± 0.9	Spoto et al. (2015)	3.8	1.30	70	$7.84^{+43.60}_{-6.64}$	0.37
Themis (L)	2.5 ± 1	Brož et al. (2013)	2.5	0.94	70	$2.49^{+12.60}_{-2.08}$	0.16
Hygiea (H)	2.0 ± 1	Brož et al. (2013)	2.0	1.0	71	$0.97^{+2.65}_{-0.71}$	0.44
Hygiea (L)	1.3 ± 1	Spoto et al. (2015)	1.3	0.82	71	$0.47^{+1.26}_{-0.34}$	0.24
Euphrosyne (H)	< 1.5	Brož et al. (2013)	1.5	1.06	67	$0.40^{+0.63}_{-0.24}$	3.55
Euphrosyne (L)	1.1–1.3 ± 0.3	Spoto et al. (2015)	1.1	0.95	67	$0.27^{+0.41}_{-0.16}$	2.58
						$\times 10^{10}$ (kg)	$\times 10^{10}$ (kg)
Hilda	∼ 4.0	Brož et al. (2011)	4.0	0.26	74	$24.5^{+73.77}_{-18.45}$	7.08
Meliboea	< 3.0	Brož et al. (2013)	3.0	0.15	75	$5.01^{+22.0}_{-4.0}$	0.44
						$\times 10^{6}$ (kg)	$\times 10^{6}$ (kg)
Pallas	< 0.5	Brož et al. (2013)	0.5	0.005	70	$2.23^{+14.68}_{-1.94}$	0.074

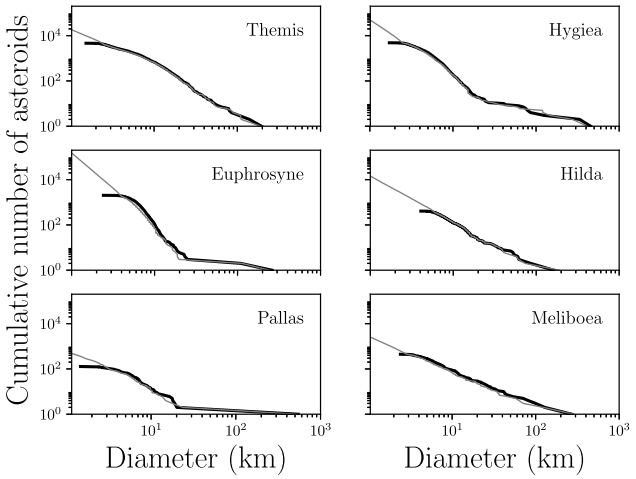

Figure 2. Observed SFDs (black line) of the six families containing members with a detected 3-μm band. Their slope (grey line) is calculated by fitting a power-law function of the diameter to the observed population with $D \geq D_{17}$, where D_{17} is the diameter that corresponds to $H = 17$, the current completeness limit of the Main Belt.

probability of obtaining one or more events from a Poisson distribution with an average success rate of five. To achieve this flux of impacts, the required number of projectiles $N_{\rm lim}$ is given by $5 = P_{\rm P} A T N_{\rm lim}$. As the number of objects (and impacts) increases with decreasing size, given the size distributions of asteroids (Fig. 2), we determine for each family the value of $D_{\rm lim}$, which is the diameter value at which the cumulative SFD of each family has a number of asteroids equal to $N_{\rm lim}$. This value of $D_{\rm lim}$, obviously, depends on the age of the family – a lower age requires a larger number of projectiles in order to achieve five impacts and thus requires extrapolation to smaller diameters (see Table 5).

The implanted mass from each family on Psyche is calculated in two steps, using a Monte Carlo procedure for the first part of the SFD for $D > D_{\rm lim}$ and an analytical method for $D < D_{\rm lim}$. For the first part of the SFD (where $D > D_{\rm lim}$), we also set an upper limit on the size of the population, D^*. The value of D^* represents the smallest impacting body that could disrupt our target Psyche catastrophically (Bottke et al. 2005). For each family used here, this limit is slightly different, as it depends on the average impact velocity that the members of each family have on Psyche (Table 4), as detailed before. We obtain the value of D^* from fig. 13 of Bottke et al. (2005), by interpolating the value of Q^*, the intrinsic energy required to disrupt an asteroid, across the curves plotted for different impact velocities and for a target having the diameter of Psyche (Table 5).

For each family, the implanted mass from the size distribution between $D_{\rm lim}$ and D^* is obtained using a Monte Carlo method. First, we extrapolate the observed size distribution from the completeness limit D_{17} to $D_{\rm lim}$ by generating a random number of synthetic bodies with a size distribution tied to the observed one and a slope α as given in Table 3. Next, we take a Monte Carlo step of 100 Myr, during which a random number is generated uniformly between 0 and 1 for each family member of the observed and extrapolated populations. If this number is smaller than $P_{\rm P} \times A \times 100\,{\rm Myr}$, then the asteroid is considered to have impacted Psyche and is removed from the simulations. In the case of an impact, we store the value of the impactor's diameter. We perform a number of steps to reach the age of the family. Once the Monte Carlo simulation is complete, we calculate the implanted mass by

$$m_{D_{\rm lim}, D^*} = f \rho \frac{\pi}{6} \sum_{i=0} D_i^3, \quad (5)$$

where i runs over the bodies that were marked as impacting. Since this is a stochastic process, involving a relatively low number of impactors, for each family we repeat each Monte Carlo run 10^4 times in order to estimate the average implanted mass and its deviation (Fig. 3). We find (Section 5) that the distributions of the implanted mass are quasi-log-normal. Therefore, we fit a Gaussian function to the occurrence distribution of $\log_{10}$ of the implanted mass, allowing us to derive the most probable value and its standard deviation, which are presented in Table 5.

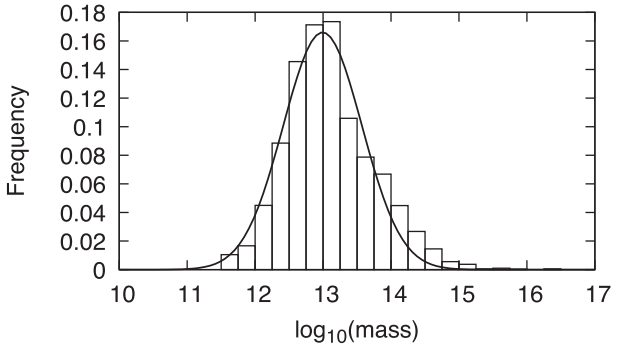

Figure 3. The result of 10^4 Monte Carlo simulations for the Hygiea family for $T = 2$ Gyr. The average implanted mass is 9.7×10^{12} kg.

For the rest of the SFD, for each source population of impactors, dN/dD is given by the size distribution of each family as described in Section 3.1. We write that

$$\frac{\mathrm{d}m}{\mathrm{d}D} = \frac{\mathrm{d}N}{\mathrm{d}D} f T A P_{\mathrm{P}} \rho \frac{\pi}{6} D^3, \tag{6}$$

which results from $\mathrm{d}M/\mathrm{d}D = \mathrm{d}N/\mathrm{d}D \times \mathrm{d}M/\mathrm{d}N$ and $\mathrm{d}M/\mathrm{d}N = \rho(\pi/6)D^3$.

From dust particles with $D = 0$ to $D = D_{\mathrm{lim}}$, the implanted mass is given by

$$m_{0,D_{\mathrm{lim}}} = f T A P_{\mathrm{P}} \rho \frac{\pi}{6} \alpha D_{\mathrm{lim}}^{-\alpha} N_{\mathrm{lim}} \int_0^{D_{17}} D^{(\alpha+2)}\, \mathrm{d}D. \tag{7}$$

This function is integrable for $\alpha > -3$ and results in the solution

$$m_{0,D_{\mathrm{lim}}} = -f T A P_{\mathrm{P}} \rho \frac{\pi}{6} \frac{\alpha D_{\mathrm{lim}}^{-\alpha} N_{\mathrm{lim}}}{\alpha + 3} D_{\mathrm{lim}}^{(\alpha+3)}. \tag{8}$$

To convert sizes to masses, we assume spherical asteroids and a constant bulk density value for all family members. We collect from the literature (Carry 2012; Fienga et al. 2014; Hanuš et al. 2017) densities of asteroids that belong to the families that mainly contribute to collisions (Themis and Hygiea) and average them. More specifically, using data for (10) Hygiea, (24) Themis, (90) Antiope, (52) Europa and (379) Huenna, we obtain an average density of $\rho = 1520\,\mathrm{kg\,m^{-3}}$. This value is also in agreement with estimates of C-complex asteroid densities from Delbo' et al. (2017). The total implanted mass is $m_{0,D_{\mathrm{lim}}} + m_{D_{\mathrm{lim}},D^*}$, summed over all the asteroid families that contribute to impacts on Psyche. In our model, the older the family, the more time this source region had to implant mass on Psyche, hence the higher the implanted mass. Since for some of the hydrated families the age is very uncertain, we calculated the implanted mass for an upper and lower limit of their ages when multiple estimations exist.

5 RESULTS

We start showing, with very simple arguments, that there is a high probability that asteroids from the Themis family alone have impacted Psyche, thus delivering hydrated/icy material. This holds when, conservatively, we restrict ourselves to the number of asteroids presently linked to the Themis family, using the family identification of Nesvorny et al. (2015). Table 4 shows that the total probability that an asteroid of the Themis family has of impacting Psyche is $7.9 \times 10^{-18}\,\mathrm{yr^{-1}\,km^{-2}}$, resulting in 1.8 impacts when the number $N = 4636$ of known family numbers is multiplied by P_{P}, the cross-section of Psyche and the upper limit of the age of Themis, $T = 3.8$ Gyr. This estimation of the number of impact events is governed by Poisson statistics and therefore the cumulative Poisson probability of having one or more impacts is 0.8347, given the 1.8 average value for impacts. The number of impacts can be even higher (2.2) when the number of family members identified by Milani et al. (2014) (AstDys download of 2017 November, $N = 5612$) is used, resulting in an impact probability of 0.8892.

Following the method described in Section 4, we calculate the implanted masses for each hydrated asteroid family. Table 5 gives our results for each part of the SFD as described in the previous section. The total averaged mass that is implanted, summed over all the source asteroid families and calculated using the maximum and minimum family ages, is in the range $m_{\mathrm{total}} \simeq 6.2$–$13.6 \times 10^{13}$ kg, meaning that, when we consider the upper age limits for Themis, Hygiea and Euphrosyne, the implanted mass is more than double. The contribution from the Themis family is between ∼40–60 per cent of the total amount, depending on its age, and that from Hygiea is ∼7–10 per cent. In addition, we see that the Euphrosyne family contributes a large amount of mass, ∼29 per cent (for both age estimates), primarily from the small-size impactors where $D < D_{\mathrm{lim}}$, which can be explained due to its steep SFD (it gives the largest number of bodies when extrapolated to small sizes). However, when we consider $D > D_{\mathrm{lim}}$, its lower P_{P} and the high value for the impact speed lead to lower implanted mass on the target, just a small fraction of that coming from Themis and Hygiea. In this calculation, we assume that the slope of Euphrosyne is constant to dust ($D = 0$), but this may not be the reality. It should be also mentioned that, according to equation (8), the mass of a family is finite for slopes greater than -3 and Euphrosyne is very close to this limit.

The Pallas, Meliboea and Hilda families contribute very little, about 1 per cent, compared with Themis and Hygiea, which are the main impactor sources on Psyche. This can be explained in several ways. First of all, the latter two families are the most numerous, with higher impact probabilities and lower impact speeds. As is shown, the mass is affected by the collisional velocity (see equation 4) and in our case Themis provides the flux of impactors with the lowest velocity.

This result is probably a conservative scenario, as the slope used for the extrapolation is the one derived from the observed population and not the initial one that each family had when it was created. This means that, especially for old families, the slope should have been steeper than the current one and thus we should lack objects from the distribution. Collisional and dynamical depletion of asteroids during the last 3.8 Gyr has removed probably about 50 per cent (or more) of the Themis initial population (Minton & Malhotra 2010; Delbo' et al. 2017). Any difference in size distribution will lead to a difference in the number of impacts and the final amount of implanted mass. Hence, ours is likely a lower limit of implanted mass. Another fact that needs consideration is that the Themis and Hygiea families, apart from being the main source of impactors, are also the contributors with the lowest impact velocities (Table 4). Therefore any Themis and Hygiea impactor should implant a higher amount of mass compared with the remaining source regions.

We apply the same technique – with some differences explained below – to the background population of asteroids with low albedo, i.e. those bodies currently unlinked to any known family. We consider only those background asteroids of the Main Belt and the Hilda population ($2.1 < a < 3.5$ au) with geometric visible albedo $p_V < 0.12$ – this threshold has been shown to include most asteroids of the spectroscopic C complex – and with $H < 17$. The latter is to avoid including asteroids below the completeness limit of the Main Belt. This results in 46 126 asteroids and the best-fitting power law to

the cumulative SFD has exponent −1.81. The observed SFD of the background asteroids starts to deviate significantly from this power-law function at $D = 3.3$ km, with the observed SFD rolling over and becoming flat, which indicates that, below this size, the sample of asteroids with measured $p_V < 0.12$ becomes observationally incomplete. Indeed, the completeness limit of the sample of asteroids with measured size and albedo is 2, 3 and 5 km for the inner, middle, and outer parts of the Main Belt, respectively (Masiero, private communication). The point at which the best-fitting power law becomes bigger than the measured SFD is at $D = 3.3$ km and $N = 38\,141$ asteroids. Assuming that these asteroids have an average intrinsic probability of impacting Psyche of 2.8×10^{-18} impact yr^{-1} km^{-2} and an average impact velocity of $v = 5.3$ km s^{-1} (the Main Belt average value: see Bottke et al. 1994), we find that the average number of impacts over the age of the Solar system (4.5 Gyr) is six, with a standard deviation of 2.4. Our 10^4 Monte Carlo simulations resulted in 6.06 ± 2.47 impacts, a result that agrees perfectly with the Poisson statistics, which give 6.08 impacts with a square root of 2.47.

The corresponding implanted mass that results from our 10^4 Monte Carlo simulations has a probability distribution with a core that is log-normal, with a high-mass tail significantly above a Gauss distribution. The best-fitting Gaussian function in $\log_{10}$(mass) versus $\log_{10}$(probability) space is centred at $\log_{10}$(mass) = 14.6, with a standard deviation of 0.4. This implies that the most likely mass implanted by the background is about 4×10^{14} kg, with the most likely range between 1.6×10^{14} and 10×10^{14} kg. The integral of the implanted mass from the background population that is smaller than $D = 3.3$ km, assuming a power-law SFD with exponent −1.81 and tied to the observed SFD, is estimated using equation (8). This results in 8.9×10^{13} kg, which is about one-fifth of the mass implanted by the observed population of the low-albedo asteroid background.

6 DISCUSSION

The understanding from the previous calculations is that Psyche has been the target of impactors originating from hydrated sources. The first outcome is that about 52–68 per cent (considering all age estimates) of the implanted mass comes from impactors with $D > D_{\rm lim}$ that have 99.9 per cent probability of producing an event. The contribution of subkillometre objects down to dust sizes corresponds to the remaining 32–47 per cent.

Here, we need to comment that it is known that families are in general bigger than those of the catalogues. However, due to the fact that the focus of their studies was to obtain a good classification of families, the authors of these works adopted a conservative approach in the selection of their quasi-random level (QRL) for the hierarchical clustering analysis (Zappala et al. 1990), in order to avoid background objects being incorrectly identified as family members and to maintain good separation in orbital elements between families.

One main question that naturally arises is whether the hydration of impactors could survive an impact of speeds representative of the Main Belt (e.g. $\langle V \rangle = 3$ km s^{-1} for Themis family impactors) and be implanted successfully on the surface of the target. Hydrocode simulations using different configurations for impacting materials, such as bulk density and composition (stony/Fe, Fe/Ni), and low impact speeds (2 km s^{-1}) show that the temperature never exceeds 150 K in extreme cases when the impacting body is pure water ice (Price, private communication). Turrini & Svetsov (2014) studied and confirmed with simulations the delivery and survival of hydrated material on Vesta from the impacting asteroid population, following several scenarios for the flux and size frequency distribution. They showed that there is an effective contamination of the target asteroid with small impactors (1–2 km in diameter). Following this work, Svetsov & Shuvalov (2015) investigated water delivery to the Moon by asteroids and comets, at higher impact speeds than the average one in the Main Belt (5.3 km s^{-1}, see Bottke et al. 1994). It was shown specifically that not only can delivery happen but the hydrated components can survive the estimated impact temperatures. Supportive of this scenario is the fact that the temperature inside a cm-size impactor's ejecta fragments cannot exceed values responsible for de-volatilization, because the exposure to extreme impact conditions is very short. Since phyllosilicates have been found in interplanetary dust particles (IDPs), this means that hydration can survive impact events, followed by ejection and atmospheric entry (Rivkin et al. 2002). This implies that hydration can also survive from the collisional events that formed asteroid families (e.g. the Ch and Cgh asteroids in the Dora and Chloris families: Bus 1999). An additional fact is that it has been shown that the 3- μm band on Murchison and other carbonaceous meteorites can be removed by exposure to higher temperatures, e.g. ∼400–600 °C (Hiroi et al. 1996). So, although an impact could partially remove ice, it is very likely that the hydrated minerals would survive collisions at such speeds.

Another aspect that needs consideration is how much of the implanted mass coming from hydrated families on Psyche (10^{14} kg) is actually hydrated and contributes to the 3- μm band. From the literature, we find that the hydration on meteorites can be up to 2–3 per cent (for CI, CM, CO, CR meteorite samples: see Rivkin et al. 2000 and references therein). In our case, this corresponds to 10^{12} kg of hydrated implanted material. However, the values of weight percentages on asteroid surfaces are lower by an order of magnitude (e.g. the values of the hydrated M-type asteroids in Rivkin et al. 2000 and references therein), an effect that could be explained by space weathering and loss of surface hydration. Can this amount excuse the observations or are more impactors needed and thus should more sources be identified? A supportive factor is that the 3- μm band on Psyche reflects two different types of hydration (Takir et al. 2017), which, although theoretically requiring aqueous alteration processes at different times or depths on the body, could also indicate different impactors. Here we show that this can be caused by the different types of impactor. Another possibility is that part of the hydration of Psyche could occur in the primordial belt, which may have been more densely populated and with a population of bodies having a different orbital dispersion.

Any impact event, besides the implantation of new material, causes erosion of the target. The ratio of erosion/implantation is affected by the impact speed. At speeds above ∼2 km s^{-1}, the erosion is always bigger than the retention of exogenous mass (Turrini & Svetsov 2014). Considering also the fact that higher impact speeds lead to higher ejecta speeds, there is a probability of exceeding the escape velocity limit and losing material in space. Therefore impacts throughout the history of Psyche implant, bury and remove any previously delivered hydration.

Psyche used to be the only large M-type asteroid that was not hydrated, being an outlier in this spectral group. Since hydration was confirmed, the boundary that was observed around 60–70 km between hydrated and non-hydrated asteroids (fig. 11 from Rivkin et al. 2000) makes even more sense than before. One explanation would be the effect of the small cross-section A of the asteroids when applied to equation (2), as large asteroids can suffer more impacts than small ones. By checking one by one the diameters of

all 48 asteroids with the 3- μm band – which belong to different spectroscopic complexes – we clearly see that that the boundary can be confirmed, with only a few exceptions (e.g. asteroids (261) Prymno and (418) Alemannia).

7 CONCLUSIONS

We study the possibility that the 3-μm band of the main-belt asteroid (16) Psyche has been caused by contamination from exogenous material. We investigate the collisional environment of the asteroid to understand which could be the hydrated sources. The Themis and Hygiea asteroid families are good potential candidates, since the hydration band has been observed in several of their members. We find that these families could contribute in total up to 10^{14} kg of foreign mass since their formation event. Investigating the potential contribution from the background asteroid population, we found that a matching amount of mass ($\sim 10^{14}$ kg) could originate from that source. However, this is not a definite conclusion, as the hydration of the background is not proven. The total implanted mass is related to the impactor's size and impact speed and the actual hydrated fraction is not yet known accurately. Further laboratory experiments are needed to estimate the hydration required in order to reproduce the observed band. The contamination due to impacts is a working hypothesis, which does not exclude either of the following scenarios for Psyche: an Fe/Ni core of a differentiated parent body or a stony/Fe body with high metal component.

ACKNOWLEDGEMENTS

In this work, we made use of asteroid physical properties data from https://mp3c.oca.eu/, Observatoire de la Côte d'Azur, whose data base is also mirrored at https://www.cosmos.esa.int/web/astphys. We thank J. Hanus for his help on asteroid masses and sizes and A. Morbidelli for his help on the collisional model. We thank the anonymous reviewer for comments and suggestions that led to significant improvement of the manuscript. This work was partially supported by the French National Research Agency under the project 'Investissements d'Avenir' UCA^{JEDI} with the reference number ANR-15-IDEX-01.

REFERENCES

Asphaug E., Reufer A., 2014, Nature Geoscience, 7, 564
Avdellidou C., Price M. C., Delbo' M., Ioannidis P., Cole M. J., 2016, MNRAS, 456, 2957
Avdellidou C., Price M. C., Delbo' M., Cole M. J., 2017, MNRAS, 464, 734
Bolin B. T., Delbo' M., Morbidelli A., Walsh K. J., 2017, Icarus, 282, 290
Bottke W. F., Nolan M. C., Greenberg R., Kolvoord R. A., 1994, Icarus, 107, 255
Bottke W. F., Durda D. D., Nesvorný D., Jedicke R., Morbidelli A., Vokrouhlický D., Levison H. F., 2005, Icarus, 179, 63
Brož M., Vokrouhlický D., Morbidelli A., Nesvorný D., Bottke W. F., 2011, MNRAS, 414, 2716
Brož M., Morbidelli A., Bottke W. F., Rozehnal J., Vokrouhlický D., Nesvorný D., 2013, A&A, 551, A117
Bus S. J., 1999, PhD thesis, Massachusetts Institute of Technology
Campins H. et al., 2010, Nature, 464, 1320
Carry B., 2012, Planet. Space Sci., 73, 98
Castillo-Rogez J. C., Schmidt B. E., 2010, Geophys. Rev. Lett., 37, L10202
Cellino A., Diolaiti E., Ragazzoni R., Hestroffer D., Tanga P., Ghedina A., 2003, Icarus, 162, 278
Daly R. T., Schultz P. H., 2015, Geophys. Res. Lett., 42, 7890
Daly R. T., Schultz P. H., 2016, Icarus, 264, 9
Davis D. R., Farinella P., Marzari F., 1999, Icarus, 137, 140
de León J., Pinilla-Alonso N., Campins H., Licandro J., Marzo G. A., 2012, Icarus, 218, 196
Delbo' M., Walsh K., Bolin B., Avdellidou C., Morbidelli A., 2017, Science, 357, 1026
DeMeo F. E., Binzel R. P., Slivan S. M., Bus S. J., 2009, Icarus, 202, 160
DeMeo F. E., Polishook D., Carry B., Moskovitz N., Burt B., Binzel R., 2015, Am. Astron. Soc., DPS meeting, 47, 301.08
Denneau L. et al., 2015, Icarus, 245, 1
Descamps P. et al., 2007, Icarus, 187, 482
Drummond J., Christou J., 2008, Icarus, 197, 480
Ďurech J. et al., 2011, Icarus, 214, 652
Elkins-Tanton L. T. et al., 2016, Lunar and Planetary Science Conference, Vol. 47. The Woodlands, Texas, p. 1631
Elkins-Tanton L. T. et al., 2017, Lunar and Planetary Science Conference, Vol. 48. The Woodlands, Texas, p. 1718
Fienga A., Manche H., Laskar J., Gastineau M., Verma A., 2014, preprint (arXiv:1405.0484)
Florczak M., Lazzaro D., Mothé-Diniz T., Angeli C. A., Betzler A. S., 1999, A&AS, 134, 463
Folkner W. M., Williams J. G., Boggs D. H., Park R. S., Kuchynka P., 2014, Interplanetary Network Progress Report, Vol. 196, p. 1
Fornasier S., Lantz C., Perna D., Campins H., Barucci M. A., Nesvorny D., 2016, Icarus, 269, 1
Gaffey M. J., Cloutis E. A., Kelley M. S., Reed K. L., 2002, in Bottke W. F., Jr, Cellino A., Paolicchi P., Binzel R. P., eds, Asteroids III. Univ. Arizona Press, Tucson, p. 183
Haghighipour N., 2009, Meteoritics and Planetary Science, 44, 1863
Hanuš J. et al., 2017, A&A, 601, A114
Hardersen P. S., Gaffey M. J., Abell P. A., 2005, Icarus, 175, 141
Hargrove K. D., Emery J. P., Campins H., Kelley M. S. P., 2015, Icarus, 254, 150
Harris A. W., 1998, Icarus, 131, 291
Hiroi T., Zolensky M. E., Pieters C. M., Lipschutz M. E., 1996, Meteorit. Planet. Sci., 31, 321
Hsieh H. H., 2014, Icarus, 243, 16
Hsieh H. H. et al., 2012, AJ, 143, 104
Jedicke R., Granvik M., Micheli M., Ryan E., Spahr T., Yeomans D. K., 2015, in Michel P., DeMeo F. E., Bottke W. F., eds, Asteroids IV. Univ. Arizona Press, Tucson, p. 795
Jones T. D., 1988, PhD thesis, Arizona Univ., Tucson
Jones T. D., Lebofsky L. A., Lewis J. S., Marley M. S., 1990, Icarus, 88, 172
Kaasalainen M., Torppa J., Piironen J., 2002, Icarus, 159, 369
Kuzmanoski M., Kovačević A., 2002, A&A, 395, L17
Magri C. et al., 1999, Icarus, 140, 379
Marsset M., Vernazza P., Birlan M., DeMeo F., Binzel R. P., Dumas C., Milli J., Popescu M., 2016, A&A, 586, A15
Masiero J. R., Mainzer A. K., Grav T., Bauer J. M., Cutri R. M., Nugent C., Cabrera M. S., 2012, ApJ, 759, L8
Matter A., Delbo' M., Carry B., Ligori S., 2013, Icarus, 226, 419
McCord T. B. et al., 2012, Nature, 491, 83
Merényi E., Howell E. S., Rivkin A. S., Lebofsky L. A., 1997, Icarus, 129, 421
Milani A., Cellino A., Knežević Z., Novaković B., Spoto F., Paolicchi P., 2014, Icarus, 239, 46
Minton D. A., Malhotra R., 2010, Icarus, 207, 744
Nesvorny D., Broz M., Carruba V., 2015, in Michel P., DeMeo F. E., Bottke W. F., eds, Asteroids IV. Univ. Arizona Press, Tucson, p. 297
O'Brien D. P., Sykes M. V., 2011, Space Sci. Rev., 163, 41
Ostro S. J., Campbell D. B., Shapiro I. I., 1985, Science, 229, 442
Rivkin A. S., 1997, PhD thesis, Univ. Arizona, Tucson
Rivkin A. S., Emery J. P., 2010, Nature, 464, 1322
Rivkin A. S., Howell E. S., Lebofsky L. A., Clark B. E., Britt D. T., 2000, Icarus, 145, 351
Rivkin A. S., Howell E. S., Vilas F., Lebofsky L. A., 2002, in Bottke W. F., Jr, Cellino A., Paolicchi P., Binzel R. P., eds, Asteroids III. Univ. Arizona Press, Tucson, p. 235

Rivkin A. S., Campins H., Emery J. P., Howell E. S., Licandro J., Takir D., Vilas F., 2015, in Michel P., DeMeo F. E., Bottke W. F., eds, Asteroids IV. Univ. Arizona Press, Tucson, p. 65
Sanchez J. A. et al., 2017, AJ, 153, 29
Shepard M. K. et al., 2008, Icarus, 195, 184
Shepard M. K. et al., 2010, Icarus, 208, 221
Shepard M. K. et al., 2017, Icarus, 281, 388
Somenzi L., Fienga A., Laskar J., Kuchynka P., 2010, Planet. Space Sci., 58, 858
Spoto F., Milani A., Knežević Z., 2015, Icarus, 257, 275
Standish E. M., Fienga A., 2002, A&A, 384, 322
Svetsov V., 2011, Icarus, 214, 316
Svetsov V. V., Shuvalov V. V., 2015, Planet. Space Sci., 117, 444
Takir D., Emery J. P., 2012, Icarus, 219, 641
Takir D., Reddy V., Sanchez J. A., Shepard M. K., Emery J. P., 2017, AJ, 153, 31
Tedesco E. F., Noah P. V., Noah M., Price S. D., 2002, AJ, 123, 1056
Tholen D. J., 1989, in Binzel R. P., Gehrels T., Matthews M. S., eds, Asteroid Taxonomic Classifications in Asteroids II. Univ. Arizona Press, Tucson, p. 1139
Tsirvoulis G., Morbidelli A., Delbo' M., Tsiganis K., 2017, preprint (arXiv:1706.02091)
Turrini D., Svetsov V., 2014, Life, 4, 4
Turrini D. et al., 2014, Icarus, 240, 86
Turrini D., Svetsov V., Consolmagno G., Sirono S., Pirani S., 2016, Icarus, 280, 328
Usui F. et al., 2011, PASJ, 63, 1117
Vernazza P. et al., 2017, AJ, 153, 72
Viateau B., 2000, A&A, 354, 725
Vilas F., Gaffey M. J., 1989, Science, 246, 790
Viswanathan V., Fienga A., Gastineau M., Laskar J., 2017, Notes Scientifiques et Techniques de l'Institut de Mécanique Céleste, 108, 1
Vokrouhlický D., Brož M., Bottke W. F., Nesvorný D., Morbidelli A., 2006, Icarus, 182, 118
Walsh K. J., Delbó M., Bottke W. F., Vokrouhlický D., Lauretta D. S., 2013, Icarus, 225, 283
Wetherill G. W., 1967, J. Geophys. Res., 72, 2429
Zappala V., Cellino A., 1996, in Rettig T., Hahn J. M., eds, Astron. Soc. Pac. Conf. Ser. Vol. 107, Completing the Inventory of the Solar system. Astron. Soc. Pac., San Francisco, p. 29
Zappala V., Cellino A., Farinella P., Knezevic Z., 1990, AJ, 100, 2030

This paper has been typeset from a TEX/LATEX file prepared by the author.